Effect of Transom Stern Bottom Profile Form on Stern Wave Resistance - An Experimental Study -*1

By Tadao YAMANO (*Member*)*2, Yoshikazu KUSUNOKI *3, Fumiyasu KURATANI *2, Takenori OGAWA *2, Teturo IKEBUCHI (*Member*)*4 and Isao FUNENO (*Member*)*4

When a ship with a wide immersed transom stern runs on a deeper draft than its design draft, forward-oriented wave breaking often occurs just behind the transom stern. The phenomenon accompanies large momentum loss and accordingly large hull resistance. The bottom profile form of the transom stern is one of the most important factors which affect the phenomenon, though not so much attention must has been paid to the part in many ships just by the reason that the part is only a limited local part of a hull. In this paper, model tests on typical bottom profile forms are conducted at first and then the effect of the bottom profile form on stern wave resistance is discussed based on the results of the model tests. As a result, characteristics and amount of the effect and the relation between the bottom profile form and the stern wave resistance are clarified.

Keywords : *Transom Stern Bottom Profile Form, Stern Wave Resistance, Model Test, Small Model Ships*

List of Symbols

B : hull breadth (m)
B_m : mean breadth of immersed transom stern end plane (m)
$C_f = R_f/0.5\rho S v_0{}^2$:frictional resistance coefficient (-)
$C_r = R_r/0.5\rho B_m I v_0^2$:residual resistance coefficient (-)
$\delta C_r = C_r - C_{r_0}$
C_{r_0} : C_r of M.S.NO.170a0a,af
$F_r = v_0/(gL_{wl})^{0.5}$: Froude number (-)
$F_{rI} = v_0/(gI)^{0.5}$: Froude number based on I (-)
g : gravitational acceleration (m/s^2)
I : stern end immersion at rest (m)
I_r : real stern end immersion at running with ship speed v_0 (m)
L_{wl} : load water line length (m)
$R_e = v_0 L_{wl}/\nu$: Reynolds number (-)
R_f : frictional resistance (N)
R_r : residual resistance (N)
R_{ts} : total resistance of a full scale ship (N)
S : wetted surface area (m^2)
v_0 : ship speed (m/s)
$v_1 = v_0(1 + 2g(I - I_r)/v_0^2)^{0.5}$: flow velocity just out of boundary layer at stern end (m/s)
δ_e : boundary layer thickness at stern end (m)
θ_e : slope angle of bottom profile at stern end (deg)
ν : kinematic viscosity of water (m^2/s)
ρ : density of water (kg/m^3)
swbf : abbreviation of 'forward-oriented wave breaking'
TKM : abbreviation of 'transverse metacentric height'

*1 平成14年11月14日造船3学会秋季連合大会において講演，原稿受付 平成14年11月20日
*2 兵庫教育大学
*3 尼崎工業高等学校
*4 川崎重工業（株）

1. Introduction

Recent container ships have rather wide immersed transom sterns to keep necessary transverse stability. When such a ship runs on a deeper draft than its design draft, forward-oriented wave breaking (abbreviated swbf hereafter)[1)2)] with high turbulent intensity often occurs just behind the transom stern. The

swbf accompanies large momentum loss and accordingly large hull resistance. To prevent or decrease the phenomenon is, therefore, important for energy saving for such ships. Some studies[3),4)] for the purpose including those on a special stern form and some appendages have been conducted by one of the authors.

However, one of the most fundamental studies to be conducted is certainly that to optimize the conventional transom stern form. In this paper, we have taken up the stern bottom profile form as a component of transom stern form to be studied, importance of which our studies[4)5)]on transom stern have suggested.

The stern bottom profile is decided in the earliest stage of hull form design. In design of the stern bottom profile form, the following two restrictions at least have to be taken into consideration. One is that by TKM and another is that by propeller vibratory forces. As shown in Fig.1, the lowest point at the stern end P1 should be lower than a point PA to keep

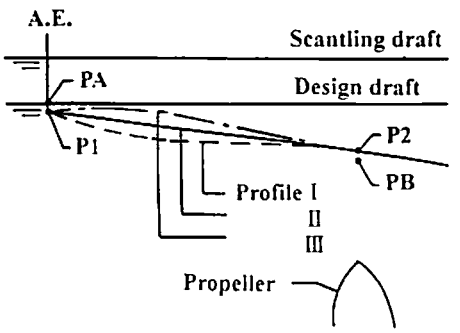

Fig.1 Restrictions to stern bottom profile form design.

necessary TKM, and the point P2 on the hull just above a propeller should be higher than a point PB to lower the propeller vibratory force under a required level. As a result, heights of two points P1 and P2 are decided. If no other restrictions are given, we can choose any form, for example, such as Profiles I, II and III shown in Fig.1 for the bottom profile between the two points. This part must has been regarded not so important for hull resistance just by the reason that it is only a limited local part of a hull, and the simplest form like Profile II must has been adopted for many ships.

As a similar study to our present study, studies[6)7)] on the effect of stern flaps or stern wedges on hull resistance have been reported. The mechanism through which the stern flaps or stern wedges reduce the hull resistance is, however, not yet completely clarified.

In the following, we compare three fundamental stern bottom profile forms, 'concave', 'flat' and 'convex' by model tests at first. Then, based on the results of the model tests, we try to clarify characteristics and amount of the effect of stern bottom profile form on stern wave resistance and the relation between the stern bottom profile form and the stern wave resistance.

2. Outline of Model Tests

2.1 Model Tests

Resistance test, stern wave height measurement and stern wave surface observation have been conducted on three model ships with different stern bottom profile forms.

2.2 Measurement Apparatus

2.2.1 Model Tank

The circulating water channel of Hyogo University of Teacher Education has been used for the model tests. Particulars of the model tank are shown in Table 1.

Table 1 Particulars of model tank.

*Length(m)	1.2
*Breadth(m)	0.3
*Water depth(m)	0.2
Flow speed(m/s)	0 - 0.7

Item with mark * shows size of observation part

2.2.2 Measurement or Observation Instruments

(1) Resistance

A new instrument has been designed and manufactured to measure the resistance of small model ships in the small model tank.

Outline of the instrument is shown in Fig.2. A model ship ① is fastened to a floating frame ②. The floating frame ② has four floats ③ (outer diameter × outer depth = 190mm × 220mm) in four water tanks④ (inner diameter × inner depth = 250mm × 220mm). The water tanks ④ are out of the model tank and on a fixed main frame ⑧. The floating frame ② is connected to the fixed main frame ⑧ with two pantographs ⑦ and is free to move fore-and-aft and up-and-down. An aimed draft of the model ship ①

can be realized by adjusting amount of the water in the water tanks ④. The floating frame ② is, on the other hand, connected to a load cell ⑥ on the fixed main frame ⑧ with a wire ⑤. The load cell ⑥ can measure resistance of the model ship ① up to 50gf. Total resistance of each of the model ships measured in the present study has ranged from 4 to 14gf.

Most of the weight of the model ship and the floating frame is supported by the buoyancy of the four floats and not by the displacement of the model ship. The model ship, therefore, can be called "a captured model ship" and not "a floating model ship".

Results of calibration for the instrument are shown in Fig.3. Fig.3 shows measurement accuracy is 0 to +2.5%.

(2) Waves

Wave heights have been measured with a servo motor type water level meter. Stern wave surface has been recorded with a digital video camera.

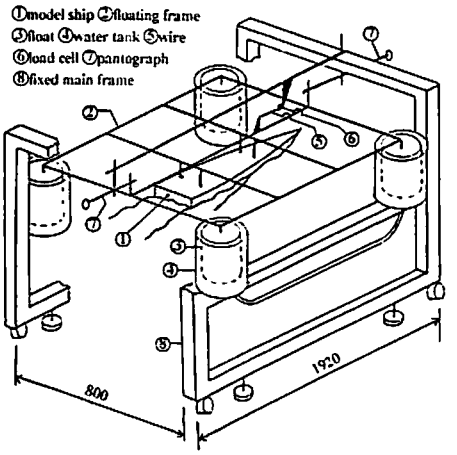

Fig.2 Resistance measurement instrument.

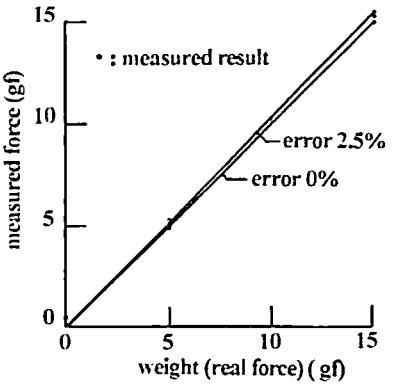

Fig.3 Results of calibration for resistance measurement instrument.

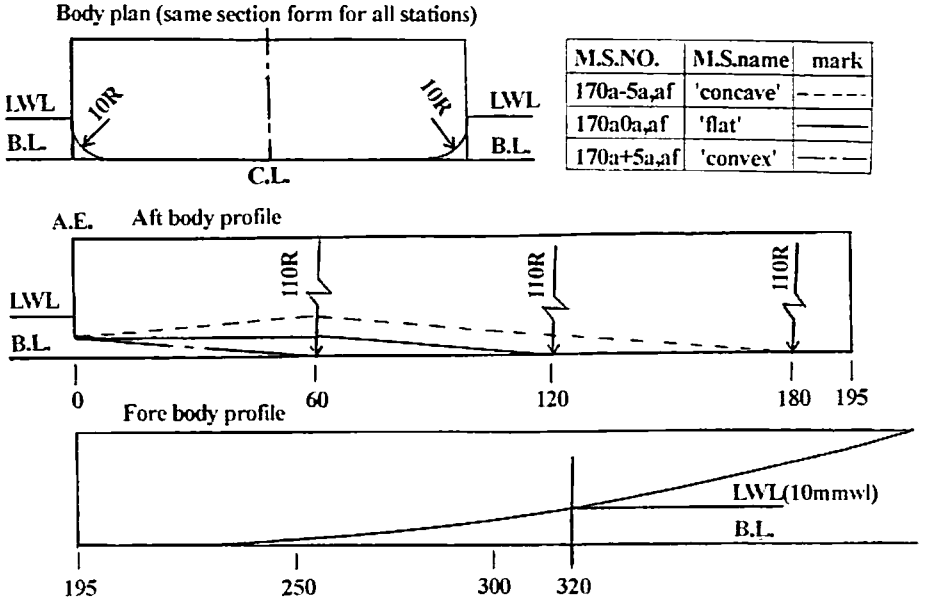

Fig.4 Hull lines of model ships

(3) Flow velocity

Flow velocity has been measured with a propeller type flow velocity meter with a 3 mm-diameter propeller.

2.3 Model Ships

Stern end immersion at rest I and slope angle of bottom profile at the stern end θ_e are important components of transom stern form for stern waves, because these two components are considered almost to determine the height and phase of the stern wave. On the other hand, θ_e can be regarded as an index to represent the stern bottom profile form. We, therefore, have designed and manufactured three model ships with different θ_e and with same I, M.S.Name 'convex' (θ_e = -4.76 deg), 'flat' (θ_e = 0 deg.) and 'convex' (θ_e = +4.76 deg.) to grasp the effect of the stern bottom profile form. Minus sign of θ_e means aft-end down and plus sign aft-end up.

Table 2 Particulars of model ships.

M.S.NO.	M.S. Name	θ_e (deg.)	L_{wl} (m)	B (m)	d (m)
170a-5a,af	'concave'	-4.76	0.32	0.1	0.01
170a0a,af	'flat'	0			
170a+5a,af	'convex'	4.76			

I(m)=0.005, B_m(m)=0.092 for all model ships.

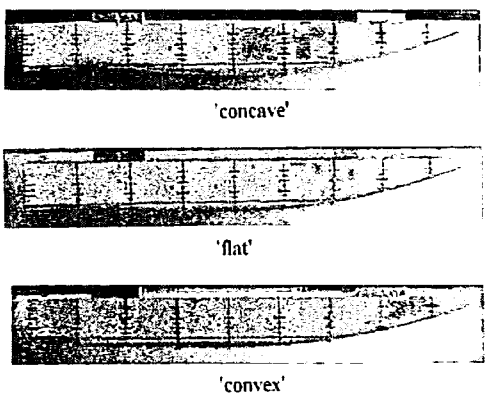

Fig.5 Photographs of model ships.

Table 2 shows particulars of the three model ships, and Fig. 4 and Fig. 5 their hull lines and photographs respectively. These model ships have same L_{wl} and same fore-bodies, and are different each other only in the stern bottom profile form.

To ensure turbulent flow stimulation, the model ships have studs of 1.5 mm height fitted with 7.5 mm intervals at the station 25 mm aft from the fore end of load water line.

L_{wl} of these model ships, 0.32 m, has been determined so that their stern waves are similar to those of 7 m long model ships based on the stern wave similarity laws proposed in refs. 8) and 9).

These model ships are used as 'a captured model ship' at the model tests as explained in 2.2.2(1). The effect of the stern bottom form on trim is, therefore, not realized at the model tests.

2.4 Test Condition

Table 3 shows test condition. Model ship speed v_0 is defined by the flow speed at 0.01 m water depth, same value as the design draft of the model ships, 500 mm fore from the tank aft end wall in the tank centerline plane, in the model tank without a model ship. Fig.6 shows water depth-wise flow speed distribution near the free surface at the position. Tested model ship speed range corresponds to the ship speed range from 18.2 to 30.3 knots (F_r=0.18-0.30) for a full-scale ship with L_{wl} of 269.2m and I of 1.8m.

3. Test Results and Discussion

3.1 Effect of Stern Bottom Profile Form on Stern Wave Resistance

Table 3 Test condition.

M.S.NO.	M.S. Name	d (m)	I (m)	$\nabla\times10^4$ (m^3)	$S\times10^2$ (m^2)
170a-5a,af	'concave'	0.01	0.005	1.642	3.718
170a0a,af	'flat'	0.01	0.005	2.223	3.881
170a+5a,af	'convex'	0.01	0.005	2.520	3.944

v_0(m/s)	0.4878	0.6091	0.6877	0.8139
F_{rI}	2.203	2.752	3.107	3.677

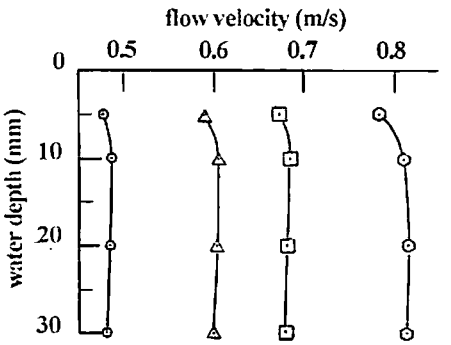

Fig.6 Flow velocity distribution in model tank without a model ship.

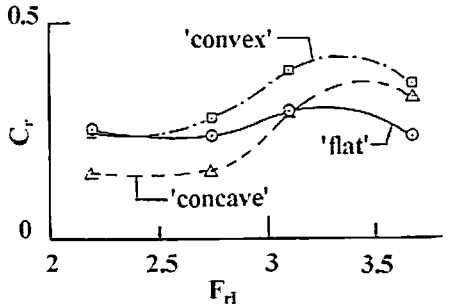

Fig.7 Resistance test results.

Fig.7 shows resistance test results, comparison of residual resistance coefficient C_r among the three model ships. To derive C_r from measured total resistance, C_f estimated by Schoenherr mean line has been used, where range of R_e is $1 - 2 \times 10^5$.

Fig.8 is derived from Fig.7 and shows the relation between θ_e and δC_r. δC_r is residual resistance coefficient difference from that of 'flat' and can be considered stern wave resistance coefficient difference due to the stern bottom profile form difference from that of 'flat', because the same fore-body form is adopted for the three model ships.

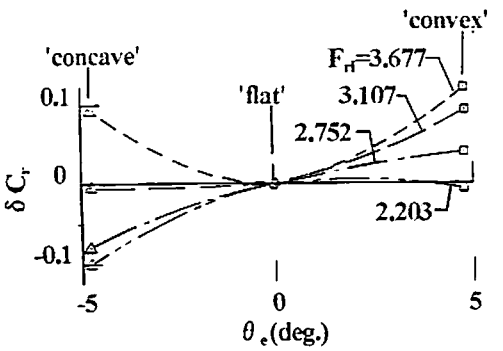

Fig. 8 Relation between slope angle of bottom profile at stern end and stern wave resistance.

The relation between θ_e and δC_r seen in Figs.7 and 8 is not so simple, and the relation can be summarized as follows: At the lowest ship speed $F_{rI} = 2.203$, stern wave resistance of 'concave' is smallest and there is no difference of stern wave resistance between 'flat' and 'convex'. At $F_{rI} = 2.752$, decrease of θ_e causes decrease of stern wave resistance. At the higher ship speed range of $F_{rI} > 3.1$, stern wave resistance of 'flat' is smallest.

3.2 Relation between Stern Bottom Profile Form and Stern Wave Resistance

3.2.1 Relation between Stern Waves and Stern Wave Resistance

Figs. 9-1, 9-2 and 9-3 show comparison of stern wave surface photographs of the three model ships taken at $F_{rI} = 2.752$, 3.107 and 3.677 respectively at the resistance tests.

Fig10 shows stern wave height comparison among the three model ships at $F_{rI} = 2.752$, 3.107 and 3.677. The stern wave heights have been measured at the points with 5mm intervals in the hull-center-line plane. The measurement has been conducted separately from the resistance test.

At the lower ship speed range of $F_{rI} < 3.1$, by comparing Figs. 9-1, 9-2 and Fig.10 with Figs.7, we can see that the stern wave surface just behind the stern end is smoother in case of lower stern wave resistance ('concave'). The smoother wave surface is considered to mean that amount of the swbf is smaller.

At the higher ship speed range of $F_{rI} > 3.1$, the relation is different. The stern wave surface of 'concave' is very smooth and almost same as that of 'flat' at $F_{rI} = 3.677$ as shown in Figs.9-3 and 10. This is considered to show that amount of the swbf and also

'concave'

'flat'

'convex'

Fig.9-1 Stern wave surface ($F_{rI} = 2.752$).

'concave'

'flat'

'convex'

Fig.9-2 Stern wave surface (F_{rI} = 3.107).

'concave'

'flat'

'convex'

Fig.9-3 Stern wave surface (F_{rI} = 3.677).

resistance due to the phenomenon are very small on both of the model ships. The stern wave resistance of 'concave' is, however, larger than that of 'flat' as shown in Figs.7 and 8.

This stern wave resistance difference between 'concave' and 'flat' is considered due to the difference of another component of stern waves, the remaining following waves[10)11)]. The remaining following waves mean the waves which do not break just behind the stern end and propagates afterwards as free waves. The remaining following wave height of 'concave' can be estimated to be larger than that of 'flat', though this tendency is not so clear in the measured wave heights shown in Fig.10.

3.2.2 Relation between Real Stern End Immersion and Stern Wave Resistance

To grasp the relation between the swbf and the stern wave resistance quantitatively, we introduce the real stern end immersion I_r defined in Fig.11. I_r is the thickness of water layer by the water broken by the swbf. Therefore, I_r can be regarded as an index to represent amount of the swbf.

I_r, on the other hand, determines the flow velocity just out of the boundary layer at the stern end v_1 according to the following relation:

$$v_1 = v_0(1 + 2g(I - I_r)/v_0^2)^{0.5} \quad (1)$$

This v_1 is one of the important factors which determine the swbf[1)2)]. The relation (1) shows that larger I_r causes lower v_1. Lower v_1 generates heavier swbf[1)2)]. So, it can also be said that I_r determines the swbf. Fig.12 shows I_r of the three model ships, in non-dimensional form, read from the record with a

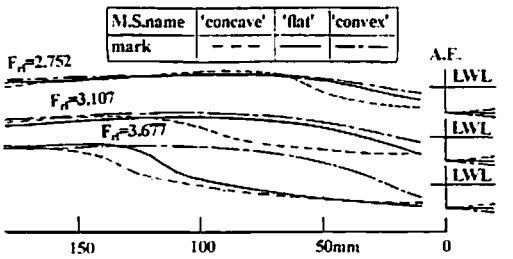

Fig.10 Measured stern wave heights.

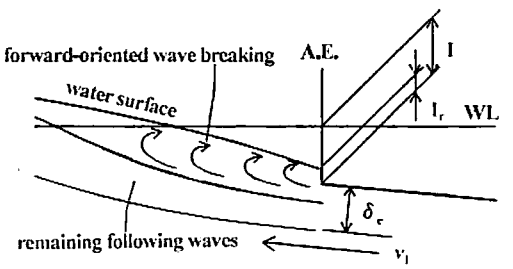

Fig.11 Definition of real stern end immersion I_r.

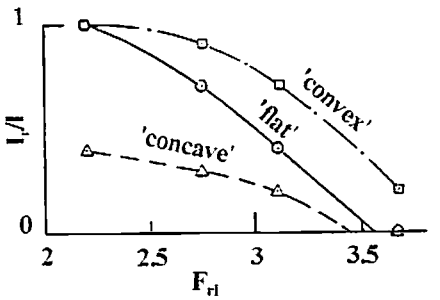

Fig.12 Measured real stern end immersion.

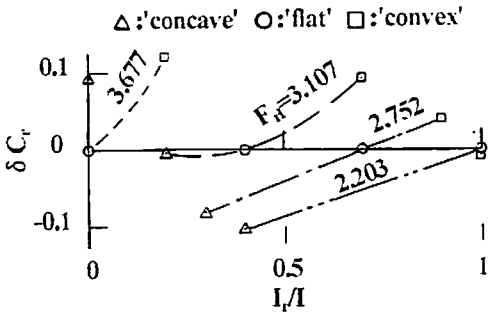

Fig.13 Relation between real stern end immersion and stern wave resistance.

digital video camera.

Fig.13 is derived from Figs.7 and 12 and shows the relation between I_r and stern wave resistance in non-dimensional form.

In Fig.13, at the lower ship speed range of F_{rI} < 2.752, we can see a close co-relation between I_r and the stern wave resistance: smaller I_r causes lower stern wave resistance. This part data in Fig.13 shows that the following test results shown in Fig.8 can be explained with the difference of I_r : No difference of stern wave resistance between 'flat' and 'convex' and the smallest stern wave resistance of 'concave' at F_{rI} = 2.203. Decrease of θ_r causes decrease of stern wave resistance at F_{rI} = 2.752. Fig.13 also confirms that the swbf largely controls stern wave resistance at the lower ship speed range[1)11)].

At the higher ship speed range of F_{rI} > 3.1, the relation is different. Smaller I_r does not necessarily bring smaller stern wave resistance. The reason has been explained in 3.2.1.

3.2.3 Relation between Stern Bottom Profile Form and Real Stern End Immersion

Fig.12 shows that I_r increases with decrease of ship speed on a stern. This confirms that the swbf is easier to occur at the lower ship speed[1)2)]. Fig.12 also shows that I_r largely depends on the stern bottom profile form and is smallest on 'concave' and largest on 'convex' at a F_{rI} .

Position of the first trough (or the trough just in front of the first peak) of stern wave is estimated to be just at the stern end in case of 'flat', that is aft from the stern end in case of 'concave' and that is fore from the stern end in case of 'convex'. This tendency can be seen in Fig10. This tendency is considered to cause the widest room between the first stern wave peak and the stern end for the water broken by the swbf of 'concave' and the narrowest room for the water of 'convex'. This size of the room is considered to be another factor to determine the value of I_r besides the amount of the swbf, the main factor.

The smallest I_r of 'concave' and the largest I_r of 'convex' at a F_{rI} are, therefore, considered to be due the largest room of 'concave' and the smallest room of 'convex'.

I_r depends on amount of the swbf and also on the stern bottom profile form as shown in Fig.12. On the other hand, I_r and not the stern bottom profile form has a close co-relation with the stern wave resistance at the lower ship speed as shown in Fig.13. These data are considered to show that I_r relates with the stern wave resistance as a cause of the swbf rather than as a result of the swbf, where I_r is a result of the swbf and is also a cause of the swbf as explained in 3.2.2.

3.3 Relative Amount of the Effect in Hull Resistance

To check whether above obtained effect of stern bottom profile form is significant in amount in the powering of a full scale ship, ratio of the stern wave resistance difference due stern bottom profile form difference to total resistance is estimated on a full-scale ship

(S.NO. CA. Full-2 condition in ref. 3) : $L_{wl} = 269.2$m, $I = 1.8$m, $d = 12.0$m) at $F_i = 0.25$, $F_{rI} = 3.057$. Stern wave resistance coefficient difference from that of 'flat' δC_r at this F_{rI} is read -0.023 for 'concave' and 0.084 for 'convex' from Fig.7. δR_r for the full-scale ship can be calculated based on these δC_r. Obtained $\delta R_r / R_{ts}$ are -3.9% for 'concave' and +14% for 'convex', where R_{ts} is total resistance of the full-scale ship. The latter value seems a little larger. However, it can be said at least that the amount of the effect is significant.

4. Conclusions

The following have been clarified by comparing three fundamental stern bottom profile forms, 'concave', 'convex' and 'flat' by model tests:

(1) Effect of the transom-stern bottom-profile form:
The concave stern bottom profile causes the lowest stern wave resistance at the lower ship speed range of $F_{rI} < 3.1$. The flat stern bottom profile causes the smallest stern wave resistance at the higher ship speed range of $F_{rI} > 3.1$.

(2) Relation between Stern Bottom Profile Form and Stern Wave Resistance:

1) At the lower ship speed rage of $F_{rI} < 3.1$, the stern bottom profile form controls the stern wave resistance mainly by controlling the real stern end immersion I_r.

2) At the higher ship speed range of $F_{rI} > 3.1$, the stern bottom profile form controls the stern wave resistance mainly by controlling the remaining following wave height.

3) The concave stern bottom profile causes the smallest real stern end immersion I_r which is important at the lower ship speed range. The flat stern bottom profile causes the lowest remaining following wave height which is important at the higher ship speed range.

(3) Relative amount of the effect in hull resistance:
Amount of the effect of the stern bottom form change is estimated to be significant in the powering for a full-scale ship.

Acknowledgements

The authors would like to thank Prof. H. Miyata, the University of Tokyo, Prof. T. Suzuki, Osaka University, Prof. T. Okuno, Osaka Prefectural University and Dr. Y. Iwasaki, Kawasaki Heavy Industries Ltd. who have cooperated with the authors in completing the subject research. The authors acknowledge that Grant-in-Aid for Scientific Research (Project No. 14550861, 2002-2003) from the Ministry of Education, Science, Sports and Culture of Japan has partly supported the subject research.

References

1) Yamano, T., Ikebuchi, T. and Funeno, I.: On Forward-oriented Wave Breaking just behind a Transom Stern, J. of SNAJ, vol.187, 2000, pp.25-32.

2) Yamano, T., Hibino, N. and Kuratani, F.: On Scale Effect of the Resistance due to Wave Breaking just behind a Transom Stern, Proc. of 7th IMDC, 2000, pp.567-577.

3) Yamano, T., Iwasaki, Y., Taguchi, K. and Maeda, N.: Development of a New Stern Form for Ocean Going Fine Ship, J. of Kansai Soc. N. A., Japan, No. 221, 1994, pp. 25-33.

4) Yamano, T., Iwasaki, Y., Taguchi, K. and Maeda, N.: Some Methods to Reduce Stern Waves, Proc. of 5th IMDC, 1994, pp.609-623.

5) Iwasaki, Y., Tahara, Y., Okuno, T., Himeno, Y. and Yamano, T.: Studies on Relationship between Water Surface behind Stern and Stern End Form of Fine Ships, J. of SNAJ, vol.180, 1996, pp.13-20.

6) Cusanelli, D.S.and Hundley, L.: Stern Flap Powering Performance on a *Spruance* Class Destroyer: Ship Trials and Model Experiments, Naval Engineers Journal, March 1999, pp.69-81.

7) Cave, W. L. and Cusanelli, D. S.: Effect of Stern Flaps on Powering Performance of the FFG-7 Class, Marine Technology, Vol.30, No.1, 1993, pp. 39-50.

8) Yamano, T., Kusunoki, Y., Kuratani, F., Ogawa, T., Ikebuchi, T. and Funeno, I.: Scale Effect of Stern Waves due to a Transom Stern - Experimental Confirmation by a New Method -, Proc. of 2nd International Workshop on Ship Hydrodynamics, 2001, pp.113-118.

9) Yamano, T., Kusunoki, Y., Kuratani, F., Ogawa, T., Ikebuchi, T. and Funeno, I.: A Method to Confirm Scale Effect of Stern Waves due to a Transom Stern, J. of Kansai Soc. N. A., Japan, No. 237, 2002, pp. 1-7.

10) Yamano, T., Kusunoki, Y., Kuratani, F., Ikebuchi, T. and Funeno, I.: On Scale Effect of the Resistance due to Stern Waves Including Forward-oriented Wave Breaking just behind a Transom Stern, Proc. of 8th PRADS, Vol.1, 2001, pp. 485-492.

11) Yamano, T., Ikebuchi, T. and Funeno, I.: On Stern Waves Consisting of Forward-oriented Wave Breaking and Remained Following Waves, J. of Marine Science and Technology, SNAJ, Vol.6, No.1, 2001, pp. 13-22.

Discussion

[Discussion] 田村欣也

コンテナ船のトランサム船尾の形状やその抵抗に就いて、理論、実験の両面から精力的に研究に取り組まれ、次々に成果を御発表になっている事に敬意を表します。

今回は小型模型船を用い、船尾プロファイル形状の相違による微量の抵抗差を巧みに検出し、その形状の影響に就いて考察した結果を御発表になりました。

以下、質問をさせて頂きます。

(1) 模型船に Turbulence Stimulator を取り付けられましたが、その取付け位置や寸法等はどのようにしてお決めになったのでしょうか。

(2) 回流水槽の水面は、模型船のない場合にも、高低差や波が生ずることがあると思いますが、波高計測の際にこれらの影響はどのように修正されたのでしょうか。 (3) 本論文の (1) 式では、文献 1) に示されている式の "I" の代わりに "$I - I_r$" を使用しています。この相違について御説明下さい。

(4) 実際のコンテナ船型に於いては通常、Fig. 1 に示されているように、船尾のプロファイルは船尾端から前方に向かって下降りとなっております。このような船型に、今回の試験結果がそのまま適用できると考えて良いでしょうか。

(5) 今回は Scantling draft を対象に試験を行っておりますが、もっと使用頻度が高い Design draft では、F_{rI} が更に大きくなると思います。このような船に対して Concave のプロファイルを採用する事に、問題はないと考えて良いでしょうか。

[Author's Reply]

ご討論有難う御座います。

(1) 回流水槽での小型模型船の実験に豊富な実績を持つ FEL の推奨を基に決めました。取りつけ位置 ss.9 1/2 近くは通常取りつけている位置です。詳細な検討を行ってはいないが、模型寸法が小さい事を考慮して、高さ 1.5mm は多少低くし、間隔 7.5mm は多少狭くした。と伺っております。

(2) ご指摘の通り回流水槽での波高計測は容易ではありません。今回の波高計測は次の手順で行っております：1) 模型船なしの状態で流速を設定して、水面がフラットとなるように（観測部最前部にある水平な波制御板の下面と水面が同一面内に入るように）水槽の水量を調整する。この時の水面を波高の基準面（波高 = 0）とする。波高計測位置の水位を計測する（ほとんど水平でした）。2) 次に模型船を設置して、模型船の排水量分だけ、水槽の水を抜く。この状態で波高を計測する。

波高計の精度に最大 +−0.1mm、波高計測前後の基準面の高さに最大 +−0.3mm の誤差が認められました。波高計測結果には、このような誤差が入っております。

(3) 現状では I_r を推定する事ができないので、文献 1) では船尾端直後の前方への波崩れが発生する直前の流れ、すなわち $I_r = 0$ の状態の流れを推定しました。それを基にして、前方への波崩れがどのように起こるかを検討しました。そこで、文献 1) では、$I_r = 0$ として船尾端での流速を推定しました。

I_r は前方への波崩れの結果ではありますが、I_r は (1) 式に従って船尾端での流速を左右します。従って、これを通して I_r は前方への波崩れを左右する原因にもなります。

今回は実験で I_r の値を計測しましたので分かっております。そこで、前方への波崩れが発生する直前の流れを推定する時に、船尾端での流速についてはこの I_r の影響を入れることにして (1) 式を採用しました。近似度を一つ上げたと言い得るかと思います。

(4) 船尾波を決める船尾端形状の主要素は I（船尾波の波高を決める）と θ_e（船尾波の位相と波高を決める）であると言う前提で今回の研究を行っております。このような前提に立てば、今回の単純な形状の模型の実験結果でも、実船の I と θ_e の検討に使えるのではないかと考えております。

但し、今回の実験では拘束模型船を使用しておりますので、船尾端形状の違いがトリムに及ぼす影響が実験結果に入っておりません。これは、別途調べる必要があります。ご指摘の前方へ向って下降りの形状は、この論文の記号を使えば、θ_e =+ deg. と定義できます。

(5) ご指摘の通り、Design draft の F_{rI} は Scantling draft の F_{rI} よりも高くなります。従って、Design draft で望ましい θ_e と Scantling draft で望ましい θ_e が異なる可能性は十分あります。両状態の船尾波による抵抗、更に両状態の航走頻度等を考慮して最適の θ_e を選ぶことになるかと思います。

[Discussion] 岡本洋

本研究は船尾端の形状、没水度、抵抗の関係について、有用な情報を示しており評価できると思います。

次の点について補足説明してください。

(1) Fig.2 の計測装置と回流水槽・水路との関係?

(2) 同じく、水タンク④との関係?

(3) Fig.12. および 13 にて、$F_{rI} = 3.677$ に於ける'concave' の点 △ は >0 のように見えるが

(4) $F_{rI} > 3.1$ にて stern-wave resistance の相関が変わるのは、3 次元影響ではないか。Stern end 幅が異なるとこの F_{rI} も異なるのではなかろうか。

[Author's Reply]

ご討論有難う御座います。

(1) および (2)

1) Fig.2 の抵抗計測装置の「固定枠」⑧, それに固定されている 4 つの「水槽」④, そして「固定枠」⑧に繋がった「筏」②, これらは回流水槽のどことも繋がっておらず, 回流水槽とは独立した装置です。「固定枠」⑧はキャスター付きで移動可能ですが, 計測時には「回流水槽」を間に挟んで跨ぐ形で両者の中心線を合わせて固定されます。

2) 「固定枠」⑧は,「筏」② を仲立ちとして, 次のような形で,「回流水槽」に浮かんだ (正確に言えば, 浮かんではおりませんが)「模型船」① に繋がっております:

· 4 つの「浮き」③ の付いた「筏」② を, 上記の 4 つの「水槽」④ に浮かべます。この「筏」② に,「回流水槽」に浮かんだ「模型船」① を個縛します。

·「模型船」① 付きの「筏」② の重量は「筏」② に付いている「浮き」③ の浮力及び「模型船」① の浮力で支えます。そこで, 模型船の喫水は 4 つの「水槽」④ の水位 (水量) を変えて調節します。この 4 つの「水槽」④ の中の, 右舷側の 2 個および左舷側の 2 個は, それぞれ水管で連結されております。

· この「筏」② を 2 つの「パンタグラフ」⑦ で「固定枠」⑧ に連結します。これにより,「模型船」① は回流水槽の中で上下および前後には動けることになります。一方で, この「筏」② を「ワイア」⑤ で「固定枠」⑧ 上の「検力計」⑥ に繋ぎます。回流水槽の水を流すと, この「検力計」⑥ が「ワイア」⑤ で「模型船」① 付きの「筏」② を引っ張る事になり, その引っ張り力すなわち模型船の抵抗を計測します。

(3)

· Fig.12 の $F_{rI} = 3.677$ の △ 点の縦軸 I_r/I の値は 0 です。ちなみに $F_{rI} = 3.677$ の ○点の縦軸 I_r/I の値も 0 です。'convex' (□) 一点鎖線の傾向から, △ 点も ○点も 3.677 より小さな F_{rI} で I_r が 0 になると推察されます。その I_r が 0 となる F_{rI} の最下点を計測はしていないので, 'flat' (○) 実線および'concave' (△) 破線の右端の形を, 'convex' (□) 一点鎖線の形状を参考にして, Fig.12 に示すような形にしたものです。

· Fig.13 の $F_{rI} = 3.677$ の △ 点の縦軸 δC_r の値は図示の通り正です。○と△はこの F_{rI} で, 両者共に $I_r = 0$ ですが, 船尾造波抵抗は○よりも △ の方が大きいと言う結果になっております。

(4) そうかもしれません。今後の検討課題とさせて頂きます。